

Steady State Solutions for a Weakly Ionised Plasma in a Sub- and Super-Sonic Axial Flow

Jonathan Blackledge

School of Electrical and Electronic Engineering
Dublin Institute of Technology
Kevin Street, Dublin 8
Ireland

Andrzej Kawalec

Department of Manufacturing Techniques and Automation
Faculty of Mechanical Engineering and Aeronautics
Rzeszow University of Technology
W. Pola 2, 35-959 Rzeszow
Poland

Abstract

The results presented in this paper relate to an application in aeronautical engineering, in particular, the use of weakly ionised plasma's to shield an aerospace vehicle from Radar by the absorption of microwave radiation. It is well known that the absorption of an electromagnetic wave with angular frequency ω over a distance x by a conductor with constant conductivity σ is determined by $\exp(-x\sqrt{\omega\mu_0\sigma/2})$ where μ_0 is the permeability of free space. The conductivity of a weakly ionised plasma is determined by its electron number density. Thus in order to evaluate the radar screening effects of a weakly ionised plasma (which is taken to reduce the Radar Cross Section of some aerospace vehicle), it is necessary to compute the steady state electron number density profile of the plasma subject to the axial flow of air over the vehicle. In this paper we consider the case of an axial flow in both the sub-sonic and super-sonic regimes obtained by evaluating the velocity potential for both cases and coupling the result with the rate equation for the plasma. This assumes that, to a good approximation, the plasma flows with the air molecules while at the same time undergoing the processes of ionisation, diffusion and recombination. It is assumed that the plasma is generated by the application of a high energy electron beam, for example, and, in this context, we consider the beam to be generated in front of the aerospace vehicle, e.g. the nose cone.

Mathematics Subject Classification:

35A22, 31C20, 35A08, 74G15, 82D10, 74F10

Keywords:

Plasma Screening of Radar, Steady State Solutions, Weakly Ionised Plasmas, Sub-sonic Axial Flow, Super-sonic Axial Flow.

1 Introduction

Aerospace stealth technologies are well known and based on two principal aspects: (i) design features; (ii) radar absorbing materials and coatings [1], [2]. The geometry of the design is based on trying to minimise those features of an aerospace vehicle that are responsible for reflecting microwave radiation in such a way that the result can fly, a principle that was not practically viable until real time digital avionic systems were available [3]. Obvious features include embedding the gas turbine engines deep into the structure of the aircraft and introducing facets - diamond shaped flat surfaces - that reflect the microwave radiation away from the source. However, one of the principal factors for reducing the Radar Cross Section (RCS) is to minimise the profile of the aircraft while maximising the ‘smoothness’ of the design as observed in the Northrop Grumman B-2 Spirit Stealth Bomber, for example [4].

Another possible approach to developing ‘stealth planes’ is through the generation of a plasma screen. The idea was first proposed by A. Eldredge in 1956 and is the basis for a US patent granted in 1964 entitled *Object Camouflage Method and Apparatus* and proposed using a particle accelerator in an aircraft to create a cloud of ionised gas that would ‘...absorb incident radar beams’ [5]. This idea has a connection with the ‘radio silence’ phenomenon that occurs during re-entry of a spacecraft. This occurs when a plasma is formed around the spacecraft due to the ‘friction’ of the Earth’s atmosphere.

The reduction of the RCS of an aerospace vehicle through the generation of a plasma requires control of plasma properties in order to design a functioning plasma stealth device. A principal property is the (carrier) frequency of an incoming Radar signal as a plasma will reflect microwaves below a certain frequency (which depends on the plasma properties) [6]. Another important aspect is how the ionised electrons travel away from the source with the air flow while simultaneously undergoing diffusion and recombination. This is an electron transport problem whose solution is required in order to evaluate the distribution of electrons (specifically the electron number density) around the skin of the vehicle away from the source, i.e. to compute the steady state distribution of the ‘plasma cloud’.

A fundamental parameter of any plasma is the ‘plasma (angular) frequency’

ω_p given by [7]

$$\omega_p = \left(\frac{4\pi n e^2}{m} \right)^{\frac{1}{2}}$$

where e is the charge of an electron (1.6×10^{-19} C), m is the mass of an electron (0.91×10^{-30} kg) and n is the number density of electrons in m^{-3} . For a plane Electromagnetic wave incident on a plasma, Maxwell's equations (for transverse EM waves) yield the dispersion relation

$$k = \frac{1}{c_0} \sqrt{\omega^2 - \omega_p^2}$$

where k is the wavenumber ($= 2\pi/\lambda$ for wavelength λ) and c_0 is the velocity of light in a vacuum ($\simeq 3 \times 10^8$ m/sec). A cut-off occurs when $\omega = \omega_p$, i.e. when there is a critical number density

$$n_c = \frac{m\omega^2}{4\pi e^2}.$$

Radio waves can only propagate through a plasma when $\omega > \omega_p$. For a typical laboratory plasma with $n = 10^{12} \text{cm}^{-3}$, a cut-off occurs when

$$f_p = \frac{\omega_p}{2\pi} \sim 10^4 \sqrt{n} = 10 \text{GHz}$$

which is in the microwave range. This effect is used as method of measuring the density of laboratory plasmas.

In principle, if an aerospace vehicle of any type, irrespective of the design, could be covered in a plasma cloud with a plasma frequency ~ 10 GHz then it would become completely impervious to detection by conventional Radar. The idea of shielding an aerospace vehicle with a self-generated plasma at an appropriate critical number density that is maintained in the presence of an airflow is not a practical proposition. However, partial plasma screening of specific features which are good radar point-scatterers is possible, one example being the point on the 'nose-cone' of a missile, for example.

In this paper, we develop the basis for a numerical simulation of a plasma that is generated by some source of electrons which ionise the air and undergo the effects of diffusion and recombination subject to a flow of air in both the sub-sonic and super-sonic regimes. The purpose of this is to compute electron density maps that simulate the steady-state distribution of electrons in order to assess the design of electron source configurations with regard to maximising the spatial extent of the screening effect. In order to contextualise the problem, we refer to Figure 1 which shows the primary and residual shock fronts generated by a X-15 travelling from left-to-right at Mach=3.5. We consider the idea that if a weakly ionised plasma could be produced where

the electrons ‘surf’ the primary shock front illustrated in Figure 1 then the aerospace vehicle could be fully impervious to detection of a ‘forward-looking Radar’ due to the absorption of this radiation from the presence of a plasma that fully ‘cloaks’ the vehicle along the cone of the (primary) shock front. The results presented in this paper represent a first attempt to investigate the viability of this concept although no specific conclusion is made in this respect.

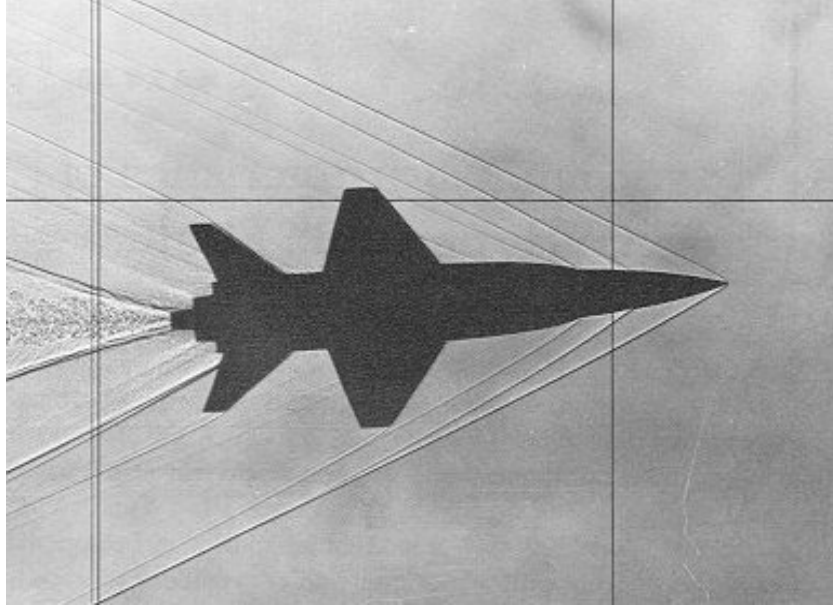


Figure 1: An X-15 travelling from left-to-right at Mach 3.5.

2 Conductivity of a Plasma

The conductivity of a plasma depends upon whether we consider it to be weakly or strongly ionised. A weakly ionised plasma is one in which the frequency of collisions ν of electrons (e) and ions (i) with atoms (a) greatly exceeds that of collisions of these particle with one another, i.e.

$$\nu_{ea} \gg \nu_{ee}, \nu_{ei}; \nu_{ia} \gg \nu_{ii}, \nu_{ie}.$$

A highly ionised plasma is described by the reverse of these inequalities.

The conductivity of a weakly ionised plasma is given by [7]

$$\sigma = \frac{ne^2}{m_e \nu_{ea}} + \frac{2ne^2}{m_i \nu_{ia}}$$

where m_e and m_i are the masses of an electron and ion, respectively. This expression for the conductivity is dominated by the first term which describes

the conductivity for the electron component of the plasma. The reason for this is that $m_i \gg m_e$ always. Clearly, in this case, the conductivity is proportional to the electron number density n and the conductivity of a weakly ionised plasma can be approximated by

$$\sigma = \frac{ne^2}{m_e\nu_{ea}} \sim 10^{-9} \frac{n}{\nu_{ea}}$$

where ν_{ea} is the frequency of collisions between electrons and atoms. In the context of the problem considered in this paper, the ratio n/ν_{ea} will vary considerably from one regime (altitude, flight speed etc.) to another, although the values of n and ν_{ea} may tend to off-set each other. Assuming that the plasma is generated by some electron beam (e-beam) breakdown of the atmosphere, at ambient atmospheric pressures, n will be large as will ν_{ea} . At higher altitudes, n will be less but so will ν_{ea} . Finally, above the atmosphere there will be relatively few atoms to break down and the collision frequency will be relatively small.

Since the conductivity of the plasma screen is linearly proportional to the electron number density, a principal problem is to determine the number density distribution for a given configuration (of source and aerospace vehicle). Thus, we are required to develop a model that predicts the generation and transport of electrons subject to a variety of processes such as ionisation, recombination, diffusion, radiative losses, air flow, etc. This can be accomplished by considering the macroscopic properties of the plasma which are governed by the dynamics of the growth process, a process that involves avalanche electron multiplication (an exponential process), i.e. the ionisation rate per initial electron. A limiting mechanism for the growth of the cascade is taken to be due to the (ambipolar) diffusion of electrons out the volume of the e-beam. Away from the plasma source, the electron number density is taken to be determined primarily by the recombination rate, radiative losses or bremsstrahlung radiation and flow regime. The ionisation mechanism is taken to include inverse bremsstrahlung processes.

3 Rate Equation for a Weakly Ionised Plasma

For electron number density n we consider the non-linear rate equation for a weakly ionised plasma given by [7]

$$\frac{\partial}{\partial t}n(\mathbf{r}, t) = B(\mathbf{r}) + In(\mathbf{r}, t) + D\nabla^2n(\mathbf{r}, t) - Rn^2(\mathbf{r}, t) \quad (1)$$

where $B(\mathbf{r})$ is the electron beam profile (which is assumed not to vary with time), I is the ionisation rate per initial electron, D is the (Ambipolar) Diffusion Coefficient of electrons and R is the Recombination Coefficient (\mathbf{r} being the spatial vector and t , the time).

The rate equation above, has two source terms and two loss terms. The source terms are B and In which describe the initial population density of electrons produced by the e-beam alone and the population density generated by the cascade process. The loss terms $D\nabla^2n$ and Rn^2 describe losses due to the processes of diffusion and recombination, respectively. Each term has a specific physical basis which is briefly reviewed in the following sections.

3.1 Electron Beam Profile

The multi-electron ionisation rate is taken to be due to an e-beam which is responsible for the production of the initial electron density from which a cascade process develops as discussed in the following section. This ionisation will depend on the distance of the beam away from the source, the beam energy, its diameter and profile. Typical parameters include an electron beam energy of 100keV, a (Gaussian) beam diameter of less than 5mm with a loss of 1keV per cm operating in air (over a range of atmospheric pressures) depending on the presence of ‘additives’ such as water vapour, for example.

3.2 Ionisation

The ionisation of a neutral gas by an electron beam, for example, is determined by a cascade process that produces an exponential growth in the electron number density. Thus, suppose that for a given volume, we require the e-beam to produce 10^{13} electrons say and that this number should be produced from an initial value of $n_0 = 10$ electrons that have been ionised by electrons from the e-beam alone, then $\ln(n/n_0) \sim 28$. In other words, the cascade process requires 28 generations to produce 10^{13} electrons from just 10 of them. This number is not strongly dependent on the assumed value of the initial density within reasonable bounds. The electron density becomes large only near the end of the cascade process; 99% of the ionisation is produced from the last 7 generations. Therefore, quantities such as the growth and losses from the cascade and the time to breakdown are determined by the conditions at times when the electron density is small.

The ionisation rate will be determined by two principal processes: the ionisation rate due to collisions of neutral atoms or molecules with electrons that have absorbed energy in the inverse bremsstrahlung process; and the loss of potential ionising electrons due to electron attachment with an ion. The process of inverse bremsstrahlung involves raising a free electron to a higher energy state in the continuum of states available to it. The energy is a result of the absorption of a photon due to bremsstrahlung radiation which is itself produced by the acceleration of charged particles involved in elastic collisions. This absorption must occur in a simultaneous interaction with a heavy particle

(atom, molecule or ion) in order that momentum is conserved.

3.3 Diffusion

Losses in electron number density due to diffusion can dominate over losses from recombination after beam initiation, and we can consider the electron density to be determined by the solution to

$$\frac{\partial n}{\partial t} = D\nabla^2 n + In.$$

For the characteristic diffusion length Λ of the breakdown, we may replace ∇^2 by $-1/\Lambda^2$ to obtain a solution of the form

$$n = n_0 \exp[(I - D/\Lambda^2)t].$$

This solution illustrates exponential growth of electrons, subject to exponential damping due to diffusion. Clearly, for a given coefficient of diffusion, the characteristic diffusion length should be low in order to achieve a high concentration of electrons.

3.4 Recombination

Electron-ion collisions may lead to recombination, i.e. the production of a neutral atom as a result of the capture of an electron by an ion. The efficiency of the processes responsible for recombination is considerable at low electron energies at which the electron-ion interaction time is sufficiently large. Accordingly, at low electron temperatures (i.e. much less than the ionisation energy) these processes strongly affect the balance of the charged plasma particles. The rate of charged particle removal due to recombination in a volume is determined by the total recombination cross section and depends of the number densities of both ions n_i and electrons n_e . Thus the rate equation is given by

$$\frac{\partial n}{\partial t} = -Rn_in_e = -Rn^2$$

where R is the recombination coefficient. The minus sign is introduced here because the process is lossy. This nonlinear equation has a simple analytical solution which can be obtained by inspection and is given by

$$\frac{1}{n} = \frac{1}{n_0} + Rt$$

where n_0 is the initial number density. After the density has fallen far below its initial value, it decays reciprocally with time, i.e.

$$n \propto \frac{1}{Rt}.$$

This is a fundamentally different behaviour from the exponential decay associated with diffusive processes and exponential growth associated with ionisation processes. Since the recombination rate is proportional to n^2 , for high values of n it can be expected to be the dominant process.

In addition to diffusion processes, the quadratic recombination term substantially affects the plasma decay, the rate equation taking the form

$$\frac{\partial n}{\partial t} = \nabla^2 n + In - Rn^2$$

or, in terms of the characteristic length of diffusion,

$$\frac{dn}{dt} = - \left(\frac{D}{\Lambda^2} - I \right) n - Rn^2.$$

The solution to this equation is [7]

$$n(t) = \frac{\left(\frac{D}{\Lambda^2} - I \right) n_0 \exp \left(It - \frac{D}{\Lambda^2} t \right)}{\left(\frac{D}{\Lambda^2} - I \right) + Rn_0 \left[1 - \exp \left(It - \frac{D}{\Lambda^2} t \right) \right]}.$$

Note that when $D/\Lambda^2 - I \gg Rn$ this solution changes into an exponential form that is characteristic of ionisation growth and diffusion decay; alternatively, when $Rn \gg D/\Lambda^2 - I$ the electron density is determined by the equation.

$$\frac{1}{n} = \frac{1}{n_0} + Rt.$$

3.5 Other Effects

Another effect that can be considered is loss through radiative processes. However, for weakly ionised plasmas, it is reasonable to assume that this effect is relatively small compared to diffusion and recombination. These losses will also be proportional to n^2 since the total power P radiated per unit volume by a plasma is given by [8]

$$P \sim 1.5 \times 10^{-38} Z^2 n_e n_i T_e^{\frac{1}{2}} \text{ (Watts/m}^3\text{)}$$

where n is in m^{-3} and T_e is in eV. Because the radiated power is proportional to the square of the atomic number Z , a low Z plasma dissipate less energy through radiation.

4 Plasma Flow

If the plasma is generated in a flow of air then, to a good approximation, we can consider the electrons to flow with the air and thus conform to the

conservation equation [9]

$$\frac{\partial n}{\partial t} = \nabla \cdot (n\mathbf{v})$$

where \mathbf{v} is the velocity of the plasma flow which is taken to be the same of the air flow. Thus, defining the velocity potential u in terms of the equation

$$\mathbf{v} = \nabla u$$

then from equation (1) we obtain the plasma flow equation

$$D\nabla^2 n + B + In - Rn^2 - \nabla \cdot (n\nabla u) = 0 \quad (2)$$

Noting that

$$\nabla \cdot (n\nabla u) = \nabla n \cdot \nabla u + n\nabla^2 u$$

and that

$$\nabla u \cdot \nabla n = \nabla \cdot (u\nabla n) - u\nabla^2 n$$

we can write

$$\nabla \cdot (n\nabla u) = \nabla \cdot (u\nabla n) - u\nabla^2 n + n\nabla^2 u \quad (3)$$

Incompressible flows conform to the Laplace equation [10]

$$\nabla^2 u = 0 \quad (4)$$

and with this result, from equation (3) we can write equation (2), in the form

$$(D + u)\nabla^2 n + B + In - Rn^2 - \nabla \cdot (u\nabla n) = 0 \quad (5)$$

Given equation (5), the problem is to find n given u which requires the velocity potential to be computed *a priori* by solving equation (4).

By computing the velocity potential for air (in the absence of a plasma) we consider a model in which the flow of the plasma is characterised by this potential alone. In other words, we consider the plasma to flow away from the plasma source (while at the same time undergoing the effects of ionisation, diffusion and recombination) in a manner that is determined by the stream lines associated with the air flow. Equation (5) is thus the steady state equation for the electron number density n subject to a flow regime characterised by velocity potential u . The velocity potential that is used in the computation of n via equation (5) depends upon the flow regime. In this paper, we consider both sub-sonic and super-sonic (but not transonic or hypersonic) flows. For small angles of attack and thin bodies, the difference is compounded, respectively, in the solution to the Laplace equation - equation (4) - and the linearised small-perturbation potential equation given by (for super-sonic axial and compressible flow along the x -coordinate) [11]

$$\nabla^2 u = M^2 \frac{\partial^2 u}{\partial x^2} \quad (6)$$

where M is the Mach number of the incoming free stream (given by the velocity of the incoming free stream divided by the speed of sound of the medium). In this case, equation (5) includes an additional term, i.e. equation (5) becomes

$$(D + u)\nabla^2 n + B + In - Rn^2 - \nabla \cdot (u\nabla n) + M^2 \frac{\partial^2 u}{\partial x^2} = 0 \quad (7)$$

Equation (6) may be recast into Laplace's equation by a simple coordinate transformation. Solutions to the Laplace equation will be considered later together with the effect of incorporating a shock front for the super-sonic case. In the following section, we consider a solution to equation (5) given that the velocity potential is known *a priori*.

5 Fundamental Solution to Equation (5)

The fundamental solution to equation (5) can be obtained by via a convolution integral with the Green's function g which is the solution of

$$\nabla^2 g(\mathbf{r} | \mathbf{r}') = -\delta(\mathbf{r} - \mathbf{r}')$$

This approach provides a solution of the form

$$n = g \otimes \left[\frac{B}{u + D} + \frac{In}{u + D} - \frac{Rn^2}{u + D} - \frac{\nabla \cdot (u\nabla n)}{u + D} \right] \quad (8)$$

where \otimes denotes the convolution integral. The dimensions of this convolution integral depends upon the dimension in which the solution is required as does the Green's function. For the three-dimensional case the Green's function is given by [10]

$$g(r) = \frac{1}{4\pi r} \quad (9)$$

and for the two-dimensional case

$$g(r) = \frac{1}{2\pi} \log(r) \quad (10)$$

where $r \equiv |\mathbf{r}|$. In either case, the solution to equation (8) requires an iterative approach. To this end, we consider a solution in which the iterations are taken to be in the same order as the physical processes that determine the characteristics of the plasma, i.e. initial electron generation by the e-beam, ionisation, recombination and flow. Thus, we consider the following iterative process:

Electron generation

$$n_1 = g \otimes \frac{B}{u + D} \quad (11)$$

Ionisation

$$n_2 = n_1 + g \otimes \frac{In_1}{u + D} \quad (12)$$

Recombination

$$n_3 = n_1 + n_2 - g \otimes \frac{Rn_2^2}{u + D} \quad (13)$$

Flow

$$n_4 = n_1 + n_2 - n_3 - g \otimes \frac{\nabla \cdot (u\nabla n_3)}{u + D}$$

The fundamental solution given by equation (8) is based on application of the following (homogenous) boundary conditions on the domain $\Omega \subset \mathbb{R}^3$:

$$n(\mathbf{r}) = 0, \forall \mathbf{r} \in \partial\Omega \quad \text{and} \quad \hat{\mathbf{n}} \cdot \nabla n(\mathbf{r}) = 0, \forall \mathbf{r} \in \partial\Omega$$

where $\hat{\mathbf{n}}$ is normal to the boundary $\partial\Omega$. These boundary conditions are consistent with the solution for the number density being taken to be in the infinite domain which in turn is consistent with the plasma generation being external to a body subject to an external flow.

For an axial flow, it is reasonable to assume that the divergence of the vector $u\nabla n$ is negligible and it is under this assumption that we may consider the evaluation of the number density n_3 alone as given by equation (13), subject to the computation of the number densities n_1 and n_2 given by equations (11) and (12), respectively. From equation (13) it is clear that the number density can be expected to decrease if the Diffusivity of the electrons and/or the Velocity Potential is large, i.e. n_1 is characterised by the reciprocal of the sum of the Diffusivity and Velocity Potential. For constant Diffusivity, the spatial distribution of the electrons will therefore be determined by the spatial variations in the Velocity Potential and in the following section, an algorithm for computing this potential is considered.

6 Evaluation of the Velocity Potential

6.1 Velocity Potential for an Incompressible Flow

For an incompressible flow, the Velocity Potential requires the solution to equation (4). Numerical solutions to the Laplace equation are common to a range of problems in fluid dynamics (e.g. [12], [13] and [14]). In this section, we consider an approach which yields a solution that is compatible with the fundamental solution to equation (5), i.e. convolution with the two- or three-dimensional Green's function for the Laplace operator.

It is well known that the Green's function solution to the Laplace equation is given by [12]

$$u(\mathbf{r}) = \oint_{\partial\Omega} [g(\mathbf{r} | \mathbf{r}') \nabla u(\mathbf{r}') - u(\mathbf{r}') \nabla g(\mathbf{r} | \mathbf{r}')] \cdot \hat{\mathbf{n}} d^2 \mathbf{r}'$$

to which we can apply the boundary condition (assuming an external flow)

$$u(\mathbf{r}) = 0, \forall \mathbf{r} \in \partial\Omega$$

Using the divergence theorem we then have

$$u(\mathbf{r}) = \int_{\mathbb{R}^3} \nabla \cdot [g(\mathbf{r} | \mathbf{r}') \nabla u(\mathbf{r}')] d^2 \mathbf{r}'$$

or, using the convolution integral operator notation,

$$u(\mathbf{r}) = g(r) \otimes \nabla^2 u(\mathbf{r}) + \nabla g(r) \otimes \cdot \nabla u(\mathbf{r}) \quad (14)$$

Equation (14) requires an iterative scheme in order to solve for the Velocity Potential u . For a flow that is external (or internal) to an object of compact support in the domain $\Omega \subset \mathbb{R}^3$, it is clear that $u(\mathbf{r}) = 0, \forall \mathbf{r} \in \mathbb{R}^3$. Suppose that

$$\nabla^2 u(\mathbf{r}) = f(\mathbf{r}) = \begin{cases} 0, & \mathbf{r} \in \mathbb{R}^3 \\ 1, & \mathbf{r} \notin \mathbb{R}^3 \end{cases}$$

We can then consider the series solution

$$u(\mathbf{r}) = [g(r) \otimes f(\mathbf{r})]f(\mathbf{r}) + \{\nabla g(r) \otimes \cdot \nabla [g(r) \otimes f(\mathbf{r})]f(\mathbf{r})\}f(\mathbf{r}) + \dots$$

the first order solution being given by

$$u(\mathbf{r}) \sim [g(r) \otimes f(\mathbf{r})]f(\mathbf{r}) \quad (15)$$

The binary function f distinguishes between the domains in which the flow can exist or otherwise where it is noted the convolution with the Green's function is over both domains. In this context, for equations (11)-(13) to be compatible with the computation of the Velocity Potential considered here, it is necessary to condition the solutions for n_1 , n_2 and n_3 by multiplication with this same binary function.

6.2 Velocity Potential for a Compressible Flow

In the context of the problem considered in this paper, compressible flows occur when the the aerospace vehicle is travelling above the speed of sound. Given, that we are confining the problem to the evaluation of n_3 - equation (13) - it is necessary to compute the Velocity Potential for a compressible flow. This requires the solution to equation (6) which can be written in the form

$$\left(\beta^2 \frac{\partial^2}{\partial x^2} + \frac{\partial^2}{\partial y^2} + \frac{\partial^2}{\partial z^2} \right) u_c(x, y, z) = 0 \quad (16)$$

where $\beta = \sqrt{|1 - M^2|}$, $M > 1$ is the Prandtl-Glauert Factor [15], [16] and u_c denotes the compressible Velocity Potential. It is then clear that we can solve equation (16) using equation (15) but where we are required to introduce the coordinate transform $x := x/\beta$ which manifests itself in terms of the Green's function that is used in equation (15). In this case, the Green's function is not symmetric but 'stretched' along the x -coordinate relative to the other coordinates.

6.3 Wave Velocity Potential

In the supersonic regime, shock waves are generated. For an object taken to be in the domain \mathbb{R}^3 , this effect can be modelled in terms of a solution to the wave equation [17]

$$(\nabla^2 + k^2)u_w(\mathbf{r}, k) = -s(\mathbf{r}) \quad (17)$$

where u_w is Wave Velocity Potential, $k = \omega/\bar{c}$ (for angular frequency ω and average speed of sound \bar{c}) and

$$s(\mathbf{r}) = \begin{cases} 1, & \forall \mathbf{r} \in \partial\Omega; \\ 0, & \forall \mathbf{r} \notin \partial\Omega. \end{cases}$$

The source function s is taken to be given by the surface of the domain \mathbb{R}^3 and thus, is characterised in terms of the gradient of the binary function f . i.e.

$$s(\mathbf{r}) = \hat{\mathbf{n}} \cdot \nabla f(\mathbf{r})$$

Each point on this surface is taken to generate a wave function, the combination of all such functions thereby generating a shock front that is determined by the 'geometry' of the source function s . The fundamental solution to equation (17) is [10]

$$u_w(\mathbf{r}) = [G(r) \otimes s(\mathbf{r})]f(\mathbf{r}) \quad (18)$$

where it is assumed that $u(\mathbf{r}) = 0, \forall \mathbf{r} \in \mathbb{R}^3$ and where G is the Green's function for the Helmholtz operator given by (for constant k)

$$G(r) = \frac{\exp(ikr)}{4\pi r}, \quad \mathbf{r} \in \mathbb{R}^3$$

and

$$G(r) = \frac{\exp(i\pi/4) \exp(ikr)}{\sqrt{8\pi} \sqrt{kr}}, \quad kr \gg 1, \quad \mathbf{r} \in \mathbb{R}^2$$

for the two- and three-dimensional cases, respectively.

In the Fresnel zone where the scale length $L > r$, these Green's functions become [10]

$$G(r) = \frac{1}{4\pi L} \exp(ikL) \exp(-ik\hat{\mathbf{m}} \cdot \mathbf{r}) \exp(i\alpha r^2)$$

and

$$G(r) = \frac{\exp(i\pi/4)}{\sqrt{8\pi kL}} \exp(ikL) \exp(-ik\hat{\mathbf{m}} \cdot \mathbf{r}) \exp(i\alpha r^2)$$

respectively, where $\hat{\mathbf{m}} = \mathbf{L}/L$ and for wavelength λ

$$\alpha = \frac{k}{2L} = \frac{\pi}{\lambda L}$$

However, noting that [18]

$$\frac{ik}{2L} |\mathbf{L} - \mathbf{r}|^2 = \frac{ik}{2L} (L^2 + r^2 - 2\mathbf{L} \cdot \mathbf{r}) = \frac{ikL}{2} + \frac{ikr^2}{2L} - ik\hat{\mathbf{m}} \cdot \mathbf{r}$$

then, ignoring scaling constants, from equation (18) we have

$$u_w(\mathbf{r}) = [\exp(i\alpha r^2) \otimes s(\mathbf{r})]f(\mathbf{r}) \quad (19)$$

Given that equation (19) ignores scaling constants and that, in practice, the Wave Velocity Potential of a shock wave is non-negative, for the purpose of simulating the combined Velocity Potential, we consider the combined field

$$u(\mathbf{r}) = \gamma u_c(\mathbf{r}) + (1 - \gamma)\{u_w(\mathbf{r}) + |\min[u_w(\mathbf{r})]|\} \quad (20)$$

where $\gamma \in [0, 1]$ determines the relative contribution of each term.

7 Results: Example Simulations

We present example simulations of the electron number density profile for the two-dimensional domain and the quasi-three dimensional domain based on software developed using a MATLAB environment [19]. The convolution operation is performed using the MATLAB function *conv2* and the option 'same' which returns the central part of the convolution. The function s required to evaluate u_w given in equation (19) is computed using a Prewitt Edge Detector which is also based on the convolution operation. Thus the principal numerical process associated with implementing the simulator is based on computing a convolution sum.

7.1 Two-Dimensional Simulation

Computation of equations (11), (12), (13) and (15) for the two-dimensional domain is based on the normalised Impulse Response Function (IRF)

$$\frac{\log(r)}{\|\log(r)\|_\infty}, \forall r \in (0_+, 1]$$

as shown in Figure 2 (left) for a 256×256 rectangular (uniformly sampled) grid. The second IRF that must be used is for the computation of u_w in equation (19). For this purpose, given that both s and u_w are taken to be real, we use the function $\cos(\alpha r^2)$ an example of which is shown in Figure 2 (right) for the case of $\alpha = 0.001$.

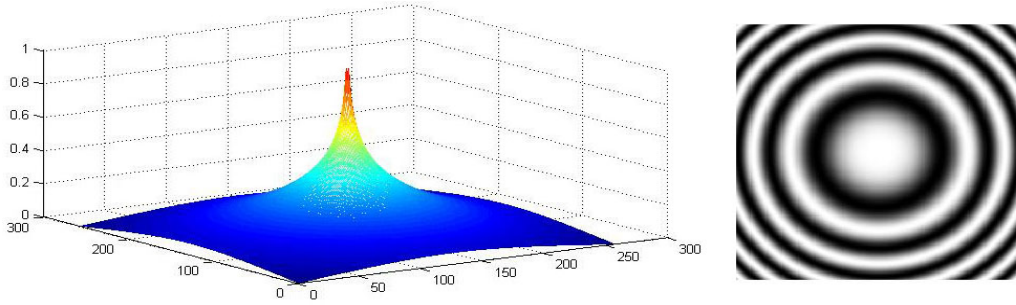


Figure 2: Left: Surface plot of the Impulse Response Function used for the two-dimensional computation of equations (11), (12), (13) and (15). Right: Impulse Response Function used for the two-dimensional computation of equation (19).

The simulation requires a binary function $f(\mathbf{r})$ to be constructed which defines the domain of the external axial flow. We consider the simple cone given in Figure 3 (left) where the flow is taken to occur in the horizontal direction and from right to left (based on a regularly sampled 256×256 grid). An initial source of electrons generated by an electron beam emanating from the tip of the cone is shown in Figure 3 (left). The beam is taken to be radially and axially uniform over its spatial extent with $B = 1$ (in practice, the electron number density of the beam may be expected to be radially Gaussian and decay along its axis as briefly discussed in Section 3.1). Figure 3 (right) provides a map of the electron number density computed using equation (13) (for $D = I = R = 1$) subject to ‘conditioning’ with the binary function f of equations (11)-(13) and where the Velocity Potential is computed using equation (15). In comparison, Figure 4 provides maps of the electron number

density using the same parameter settings but for the case of a compressible flow using equation (20) for $M = 2$ and $M = 3$ with $\alpha = 0.001$ and $\gamma = 0.01$. The result shows the emergence of a bifurcation from the source in which the maximum number density becomes separated from the beam axis.

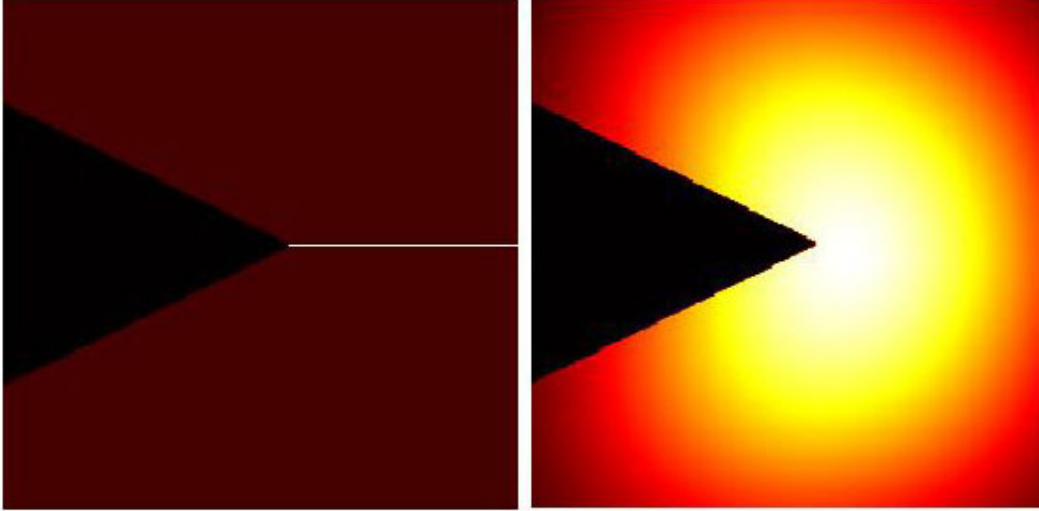


Figure 3: Left: Configuration of the nose cone (black) and uniform electron beam. Right: Electron number density computed using equation (13).

7.2 Quasi-Three-Dimensional Simulation

Simulating three dimensional flows is computationally intensive and is not addressed in this paper. However, in order to investigate three-dimensional effects in the context of the methods and results given in the previous section, and, under the assumption that the airflow is radially symmetric, we consider the case when the binary function f is taken to be an infinitely thin slice in the xy -plane thereby allowing us to write $f(x, y, z) = f(x, y)\delta(z)$. From equation (15), it is then clear that we have

$$u(x, y, z) = \left[\frac{1}{4\pi\sqrt{x^2 + y^2 + z^2}} \otimes f(x, y) \right] f(x, y)\delta(z)$$

where \otimes is taken to denote the convolution integral over x and y only. If we then consider the computation of u at $z = 0$ we obtain

$$u(x, y) = \left[\frac{1}{4\pi\sqrt{x^2 + y^2}} \otimes f(x, y) \right] f(x, y)\delta(0)$$

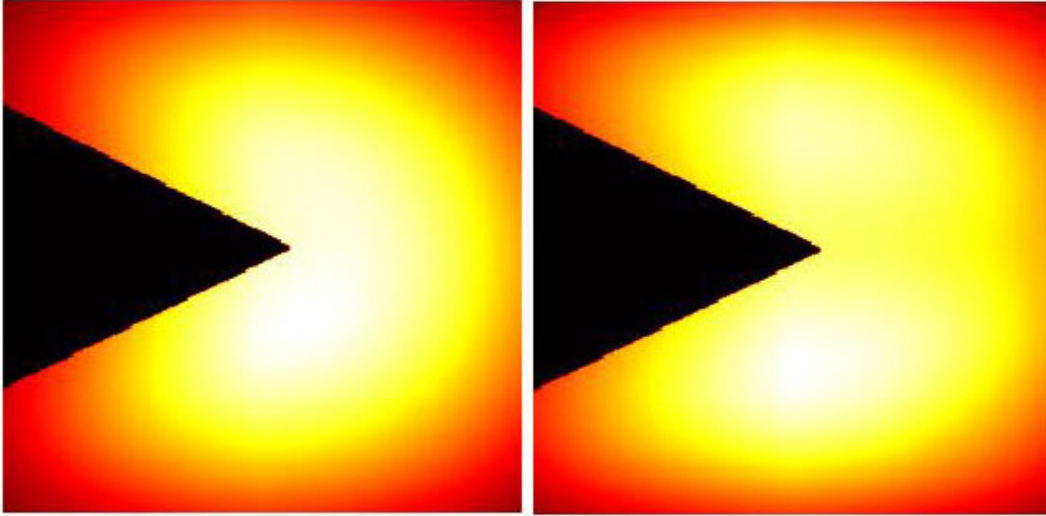


Figure 4: Left: Electron number density for $M = 2$. Right: Electron number density for $M = 3$.

Similarly, with $B := B\delta(z)$, $I := I\delta(z)$, $R := R\delta(z)$, the evaluation of equations (11)-(13) at $z = 0$ becomes predicated on a two-dimensional convolution where

$$g(x, y) = \frac{1}{4\pi\sqrt{x^2 + y^2}}$$

This three-dimensional to two-dimensional transformation allows us to consider an identical simulation procedure to that described in the previous section except that the IRF now takes the normalised form

$$\frac{r^{-1}}{\|r^{-1}, \|\infty} \forall r \in (0_+, 1]$$

By way of an example, we show an effect that is not evident in the two-dimensional simulation for the same parameter settings and the same beam profile (as given in Figure 3). This is provided in Figure 5 which illustrates the influence of the wave pattern on the electron number density using this Quasi-Three-Dimensional (Q3D) approach. The localisation of the electron number density shown in this figure either side of the cone is due to the presence of a standing node where the Velocity Potential associated with the shock wave forms a local minimum. This is an example of the possibility for electron transport to provide a plasma screen that is spatially distinct from the locality of source.

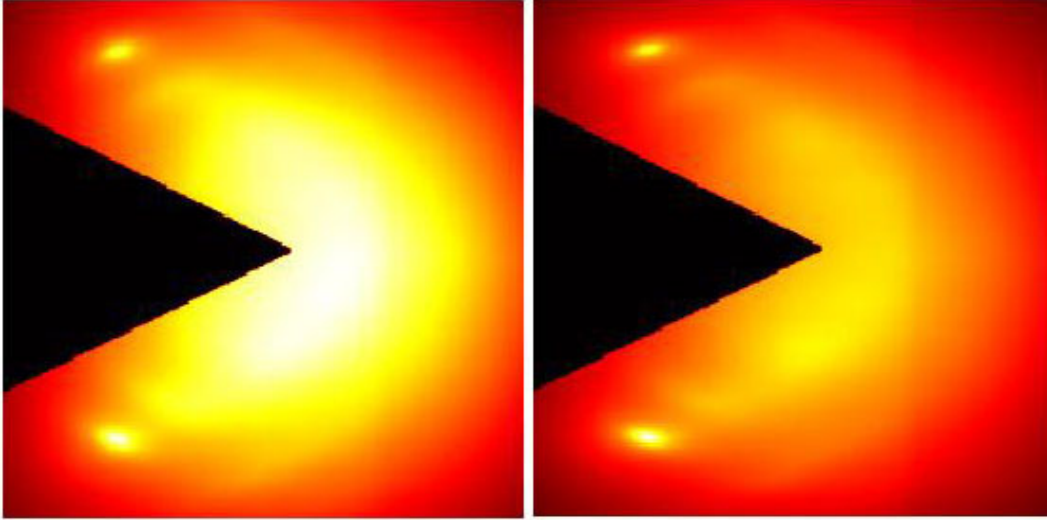


Figure 5: Left: Q3D electron number density for $M = 2$. Right: Q3D electron number density for $M = 3$.

8 Conclusions

The application of aerospace plasma screening relies on a weakly ionised plasma in which the conductivity of the plasma is determined by the electron number density of the plasma. However, a very weakly ionised plasma can still significantly reduce the RCS. For a plasma with a conductivity of say 1 siemens/metre, the skin depth is 1 mm, i.e. the length over which the electric field strength has decayed by \exp^{-1} or by $\sim 63\%$. The basic problem is to understand how the plasma is distributed over the skin of an aerospace vehicle from its source in the presence of air flow. It is intuitive to assume that as the plasma streams away from the source the effects of airflow, diffusion and recombination will significantly reduce the electron number density. This is evident from the simulations that have been presented in Section 7 for a pencil line e-beam.

The extent of the plasma sheath that forms over the immediate boundary of the nose cone is quite noticeable when air flow is present, an extent that is strongly determined by the magnitude of the recombination coefficient and air flow for a given beam energy and coefficient of ionisation. Actual values for R along with I , D and the beam profile B (which will not be uniform as in the idealised simulations presented here) and the flow rate depend on the operating conditions that apply. These include the aerospace vehicle velocity, the plasma medium, additives (readily ionisable or reactive species), the electron beam energy, its diameter and profile.

In the supersonic case, there is evidence that the electron number density profile is influenced by the wave patterns generated by the shock front in the

locality of the source (for the Q3D case). However, it remains to be understood whether it is possible to generate a more extensive plasma screen based on electrons surfing the shock front further away from the source. It may be expected that the plasma is partially distributed along the shock front and thus, depending on the exact configuration of the aerospace vehicle, provide a more extensive plasma screen. In this context the spatial distribution and direction of the source is significant. Possible applications may include the plasma screening of in-coming missiles, for example, against close proximity anti-missile systems that use radar for targeting and control [20].

Acknowledgements

The authors would like to acknowledge the support of the Science Foundation Ireland and the National Science Centre, Poland.

References

- [1] J. Jones, *Stealth Technology: The Art of Black Magic*, AERO 1989, ISBN: 978-0830682812.
- [2] P. A. Suhler, *From RAINBOW to GUSTO: Stealth and the Design of the Lockheed Blackbird*, AIAA, 2009, ISBN: 978-1-60086-712-5.
- [3] C. R. Spitzer, *Digital Avionics Systems*, Prentice-Hall, 1987, ISBN: 978-1930665125.
- [4] A. Alexeev, E. Shtager and S. Kozyrev, *Physical Foundation of Stealth Technology*, Saint-Petersburg, VVM Ltd Publishing, 2007.
- [5] A. Eldredge, *Object Camouflage Method and Apparatus*, US patent 3127608, August 6, 1956, issued March 31, 1964.
- [6] J. R. Wait, *Electromagnetic Wave Theory*, Harper and Row, 1985. ISBN: 9-780-06046877-4.
- [7] V. E. Golant, A. P. Zhilinsky and I. E. Sakharov, *Fundamentals of Plasma Physics*, Wiley series in Plasma physics, 1977, ISBN: 9-780-47104593-9.
- [8] K. Nishikawa and M. Wakatani, *Plasma Physics* Third Edition, Springer, 2000, ISBN: 3-540-65285-X.
- [9] G. K. Batchelor, *An Introduction to Fluid Dynamics*, Cambridge University Press, 1967, ISBN: 0-521-66396-2.

- [10] G. A. Evans, J. M. Blackledge and P. Yardley, *Analytical Methods for Partial Differential Equations*, Springer, 1999 , ISBN: 3-540-76124-1.
- [11] P. Balachandran, *Fundamentals of Compressible Fluid Dynamics*, Prentice-Hall, 2010, ISBN: 978-8120328570.
- [12] G. A. Evans, J. M. Blackledge and P. Yardley, *Numerical Methods for Partial Differential Equations*, Springer, 1999, ISBN: 978-3540761259. Springer, 2000.
- [13] Wolfram Mathematica 9 Document Centre, *Numerical Solution of Partial Differential Equations*, Mathematica Tutorial, 2014, <http://reference.wolfram.com/mathematica/tutorial/NDSolvePDE.html>.
- [14] S. Salsa, *Partial Differential Equations in Action*, (The Laplace Equation, pp. 102-155), Springer, 2008, ISBN: 978-8847007512.
- [15] A. M. Kuethe and C. Y. Chow, *Foundations of Aerodynamics*, Wiley, 1976.
- [16] A. H. Shapiro, *Compressible Fluid Flow*, Wiley, 1953.
- [17] F. B. Jensen, W. A. Kuperman., M. B. Porter and H. Schmidt, *Computational Ocean Acoustics*, Chapter 2: Wave Propagation Theory, pp. 65-153, Springer, 2011, ISBN 978-1-4419-8678-8.
- [18] J. M. Blackledge and B. Babajanov, *Three-dimensional Simulation of the Radiation Field Patterns Generated by an Integrated Antenna*, IAENG, International Journal of Applied Mathematics, Vol. 43, No. 3, 1-16, 2013.
- [19] MathWorks, *MATLAB*, 2014, <http://www.mathworks.se/products/matlab/>.
- [20] Raytheon, *Phalanx Close-in Weapon System*, <http://www.raytheon.com/capabilities/products/phalanx/>